Simulating Nanomaterial Transformation in Cascaded Biological Compartments to enhance the Physiological Relevance of *In Vitro* Dosing Regimes: Optional or Required?

Samantha V. Llewellyn, Angela Kämpfer, Johannes G. Keller, Klaus Vilsmeier, Veronika Büttner, Didem Ag Seleci, Roel P. F. Schins, Shareen H. Doak* and Wendel Wohlleben*

Samantha V. Llewellyn and Shareen H. Doak*

[1]*In vitro* Toxicology Group, Institute of Life Science, Swansea University Medical School, Swansea University, Singleton Park, Swansea SA2 8PP, Wales, UK.

Email*: S.H.Doak@swansea.ac.uk

Johannes G. Keller, Klaus Vilsmeier, Didem Ag Seleci and Wendel Wohlleben*

[2]Advanced Materials Research, Dept. of Material Physics and Analytics and Dept. of Experimental Toxicology and Ecology, BASF SE, 67056 Ludwigshafen, Germany

Email*: wendel.wohlleben@basf.com

Angela Kämpfer, Veronika Büttner and Roel P. F. Schins

[3]IUF - Leibniz Research Institute for Environmental Medicine, Auf'm Hennekamp 50, 40225 Düsseldorf, Germany

Keywords: nanomaterials; physico-chemical characterisation; ENM pre-treatment; gastro-intestinal digestion; *in vitro* hazard assessment

Abstract

Would an engineered nanomaterial (ENM) still have the same identity once it reaches a secondary target tissue after a journey through several physiological compartments? Probably not. Does it matter? ENM pre-treatments may enhance the physiological relevance of *in vitro* testing *via* controlled transformation of the ENM identity. We demonstrate the implications of material

transformation upon reactivity, cytotoxicity, inflammatory and genotoxic potential of Ag and SiO_2 ENM on advanced gastro-intestinal tract cell cultures and 3D liver spheroids. Pre-treatments are recommended for certain ENM only.

1. Introduction

When a human body assimilates a particle *via* inhalation or ingestion, that particle can translocate to secondary tissues where it might induce biological change, adaptive or adverse. During translocation, the original 'pristine' engineered nanomaterials (ENMs) are often transformed in a manner that may result in changes to surface chemistry, protein corona, morphology and dissolution.[1,2,3] At the very least, opsonins adsorb to form a corona,[3] which may form rapidly e.g. in human blood plasma, and may not change much with prolonged incubation.[4] It has been demonstrated that some fraction of that corona is "soft", in the sense of being reversible, and another fraction is "hard", and thus represent a permanently adsorbed layer around the core particle.[5] Here we draw the attention to "even harder" transformations that affect the core particle. Each biological compartment imposes different pH conditions, offers reaction partners to support reductive or oxidative transformation, and opsonins can favor aggregation by bridging or deagglomeration by colloidal stabilization **(Figure 1).** Colloidal stability, dissolution and aggregation are characteristics frequently transformed, especially under varying pH conditions as experienced in the gastro-intestinal tract (GIT).[6] Different pH solutions can have significant affects upon the surface chage, redox potential and subsequent aggregation and dissolution of Ag ENMs.[7] In an acidic or neutral pH, Ag ENMs destabilized following oxidative dissolution resulting in a greater release of ionic silver and a higher rate of aggregation. Yet, when the pH increased and became more alkaline, the ENMs restabilized in the presence of hydroxy ions.[7,8] As a result, these modifications, permanent or reversible, will transform the particle and give rise to an ENM with very different physico-chemical identities. Subsequently, this affects how the materials interact with biological systems, influencing their cellular uptake and toxicological profile.[9] For example, a sulfidised or oxidised layer on a metal ENM can passivate the biological

activity, and can slow down dissolution which in turn mediates ion toxicity. Specifically for Ag ENMs the oxidative dissolution into Ag^+ cations can result in disruption of mitochondrial function, which impacts homeostatic regulation of oxidative stress and cytokine release.[6] More often than not, this oxidative response is the primary mechanism behind Ag ENM associated cytotoxicity, DNA damage and genotoxicity, elevated immunological responses and even cell death across multiple human cell lines.[10,11,12,13,14,15] It is evident that when assessing ENM toxicity, the physico-chemical properties and transformation capability (*e.g.* dissolution, aggregation and reprecipitation) of the materials must be well defined, both before and after translocation through the body in order to fully understand the potential mechanisms of toxicity at play.

The liver is the most common secondary site for bioaccumulation following ENM entry into the body. ENM need to traverse multiple biological barriers from their site of exposure before reaching the liver and so this organ is highly unlikely to be exposed to pristine ENM. Despite this, studies evaluating ENM hepatotoxicity only utilise pristine materials and the impact of ENM biotransformation on the subsequent biological resonse is poorly understood. To overcome this, several authors have devised pre-treatments to induce a transformation towards an "aged" or "digested" or "pre-treated" ENM before *in vitro* dosing. In pulmonary toxicology, the incorporation of simulant fluids to better mimic the *in vivo* environment and biological interactions was first introduced in the mid-1980s.[16,17] Similarly pre-treatments with artificial digestion fluids have been applied for decades in the context of food research,[18,19] yet they have only recently been integrated into ENM safety assessment.[20,21] Biotransformation of ENM has even been touted as critical step in clinical translation of nanomedicine.[22] For example, digestion of Ag ENM influenced their dissolution properties and uptake in differentiated Caco-2/HT29-MTX cells, representing the intestine.[23] Current literature primarily addresses ENM biotransformation in relation to physico-chemical characterization or the effects of specific biotransformation factors (*e.g.* pH, protein composition and ionic charge) upon translocation, cellular internalization and toxicological effects of ENM. However, the cascade of

ENM transformation from site of exposure through to secondary organ systems and the direct toxicological impact of such material modifications is yet to be fully evaluated.

To address this, the approach employed in the present study was to firstly expand the pre-treatment concept that mimics the *in vivo* journey to an array of pulmonary and oral uptake scenarios (Figure 1) whereby, ENMs were incubated in one relevant medium or sequentially in up to three media (**Table S1**). Later, the pre-treated (PT) ENM were characterised and dosed onto *in vitro* models emulating both primary and secondary organ systems (*i.e.* the gastrointestinal tract (GIT) and liver respectively). Hereafter, we critically assessed the general necessity of pre-treatment schemes, which to date has primarily been used for Ag ENMs in oral ingestion scenarios. The sequential pre-treatments were demonstrated on two forms of silver (Ag) and silica (SiO_2) ENMs; both of which differed significantly in their reactivity and were meant to represent zero-valent metals and metal oxides respectively (**Table S2**, **Figure S1**). In the recent transformation framework by Gray *et al*, they represent transformation by "oxidative dissolution" (Ag) and "non-redox transformation (hydrolytic, acid-base)" (SiO_2).[24] The assays we adopted assess the concept of pre-treatment schemes from physical-chemical characterisation and abiotic reactivity testing aspect up to *in vitro* co-cultures and 3D organ models.[25] The incorporation of relevant physiological factors like, components of the digestion process or the addition of resident immune cells, has been suggested as an important consideration for intestinal and hepatic *in vitro* nanosafety testing, respectively.[26,27] Utilizing three cell lines that compose an advanced GIT model and the HepG2 spheroid liver model,[28] multiple toxicological endpoints (*e.g.* cell viability and functionality, cytotoxicity, (pro-)inflammatory response and genotoxicity) can be assessed following exposure to pristine and PT ENMs to determine if ENM GIT exposure pre-treatments are a necessary step to improve the predictive capabilities of *in vitro* test systems for ENM hazard assessment.

2. Results and Discussion

2.1 Demonstration on exposure identity

We first analysed transformation in a single compartment, specifically the gastrointestinal tract (GIT). Most transformation is likely to take place on the surface of the particles, therefore X-ray photoelectron spectroscopy (XPS) was applied with line shape analysis. Ag particles have shown transformation after the sequential gastric and intestinal (IUF) pre-treatments (**Figure 2**). Overall the silver oxidation state varied significantly between both tested silver materials. We found Ag Sigma to truly consist of metallic silver, whereas Ag NM300 showed mostly organics (73% Carbon) and only oxidized species (Ag_2O, AgO) even before any treatment (**Figure S2**). The predominance of organics must be attributed to the colloidal stabilisation by the PVP polymer coating, and the state of oxidation may be related to the several years of storage in the JRC repository, despite filling vials under Argon. Triplicate measurement of Ag Sigma did not show any significant differences between powder versus aqueous dispersion that was then dried again for XPS analysis. However, after GIT pre-treatment we observed increased amounts of Ag_2O and AgO species (Figure 2). This showed that the pre-treatment can induce expected transformation by oxidative processes. In contrast, Ag NM300 after GIT treatment only exhibited organics with little or no detectable Ag on the surface. This transformation would occur following oral exposure even before intestinal uptake or translocation into systemic circulation. At this point one would recommend that pre-treatments are relevant for materials that are susceptible to oxidation (such as zero-valent metals). Changes of dosimetry and toxicity of the ions, relased by the oxidative dissolution, would be equally important in this case.[24] When measuring the ion concentration by ICP-MS (**Table S3**), Ag Sigma showed limited response to any specific media except LSF.

We then proceeded to simulate pathways through several biological compartments. Ag Sigma generated significantly more ions in the combination of Lung Simulant Fluid (LSF) – Foetal Bovine Serum (FBS) and Gastric & Intestinal Digestion Simulant Fluids (IUF) – Phagolysosomal Simulant Fluid (PSF), but not in the sequences of FBS-PSF or IUF-FBS (Table S3). Among these sequential pre-treatments, LSF-FBS simulated the pathway of passing the air-blood barrier from lung lining

fluid to serum, and IUF-PSF simulated the passage through the stomach and intestine prior to lysosomal uptake, *e.g*. in Peyer's patches. The dissolution was not driven by a single reaction partner, otherwise it would have occurred in one media alone. Yet, such a strong dependence on medium sequences was not observed for the other Ag nanoform.

In addition to the chemical speciation of the particle surface and the release of ions, the physical structure of particles and their agglomerates can also transform. The TEM analysis before and after the aggressive IUF treatment was suggestive of an increase in polydispersity of Ag NM300 (Figure S1d) and f)). However, a statistical analysis of the particle size distributions by fractionating methods showed that the overall variation was very low for Ag NM300 (always dispersed) and also for SiO_2 NM200 (always agglomerated), (**Figure 3**, **Table S4**). In contrast, Ag Sigma and amorphous SiO_2 exhibited a 10-fold range in variation, but the TEM scans (Figure S1) show that only the agglomerate structure changes, and not the primary particles. It was only for these two ENM that the expected influence of the dispersion medium onto the state of ENM agglomeration was confirmed.[29,30] The serum proteins in FBS stabilized Ag Sigma better than any other media, whereas this was not observed for amorphous SiO_2 . Only Ag NM300 remained stable in any single or sequential pre-treatment (**Table S5**), and was the only ENM tested with sub 1nm fraction (details not shown). This was attributed to the generation and stabilization of Ag ions by organic complexes, which have been previously reported by Bove *et al*. when studying the oral dissolution of Ag NM300.[31,32] Amorphous SiO_2 dispersed to significantly smaller agglomerate sizes than SiO_2 NM200, with the exception of PSF (Table S5**)**.

We then again proceeded to simulate pathways through several biological compartments. After sequential incubations, we applied the same size distribution analysis, as described in **Table 1**. The detailed results for two Ag and two SiO_2 materials are given in Table S5, with one of each material plotted in Figure 3. Ag NM300 (Figure 3A) had a resilient colloidal stabilisation that resisted any agglomeration. The slight shift of the red solid line (incubation in FBS only) towards smaller

diameters is the tell-tale signal of opsonisation (corona formation) leading to a lower effective density and thus seemingly smaller particles in the AUC technique.[33,34] Only the dispersion directly in LSF induced minor agglomeration (see Figure 3a, black dash-dotted line), but none of the sequential incubations modulated the D50 (Table S5). This was also obvious in the median D50 values in mass metrics (Table S5). As expected from its tendency to oxidize, Ag Sigma was colloidally unstable (full distributions not shown, but **Table S6** provides median size D50 in mass metrics). The results were more complex for amorphous SiO_2 (Figure 3B), but for simplification one can normalize the median diameter after sequential incubation by the median of the size distribution when dispersed directly into the second medium (Table S6). The resulting normalisation (**Table 2**) evidenced that for amorphous SiO_2 the state of agglomeration after sequential incubation was similar to that created by dispersing directly into the second medium (white colour code in comparison to second medium in Table 2). The same was observed for the SiO_2 NM200 material.

Thus, for SiO_2 and possibly other metal oxides, with limited options of chemical transformation, the sequential incubation is an unnecessary complication of sample preparation, as it leaves little trace on the material. The same result would be obtained by directly dispersing the material into the relevant cell media. In contrast, a reactive material, such as Ag Sigma, showed large differences induced by sequential incubation compared to that observed in a single medium (blue and red color codes in Table 2). The material remains frozen in an agglomerated state induced by the first medium (illustrated in Table 2 by color intensity, where more intense colors indicate greater agglomeration). This implies for a reactive material, that the exposure identity is formed by the pre-treatment regimen, which represents an approach to design "what ENM" is exposed to the cells. However, even for Ag this cannot be generalised: the counter example is Ag NM300, which is chemically oxidised already and colloidally stabilized by polymers (Figure S2), such that only the release of ions leaves a trace of the pathway through the compartments that were simulated.

In the following sections, we focus on the pre-treatment, simulating the well-established conditions of digestion, by the sequential IUF_G and IUF_I incubations. Based on the physico-chemical transformation, it is unlikely that this GIT pre-treatment would significantly modulate the biological interactions of amorphous SiO_2; but it is possible that the digestion changes the effects of Ag.

2.2 Implications for reactivity

The reactivity of amorphous SiO_2 and Ag Sigma without and with the IUF GIT pre-treatment was measured by the FRAS assay (**Figure 4**). Amorphous SiO_2 showed similar reactivity with and without IUF GIT pre-treatment. This is an important finding, because a priori the pre-treatments may change the relative abundance of silanol and siloxane functionalities.[35] A transformation of aggregate structure, which we cannot clearly confirm under TEM (Figure S1), was thought to be induced by a destabilized siloxane network.[36] We find that the extent of that change is not enough to fundamentally alter the surface reactivity of silica that is relevant for biological oxidative damage. However, a significant difference was observed between GIT PT and pristine Ag Sigma particles, whereby the pre-treatment caused the reduction of ROS production on Ag Sigma. This was attributed primarily to the oxidation of the Ag surface (Figure 2), because the changes in the state of agglomeration are not critical in the abiotic FRAS assay.

2.3 Demonstration on Cytotoxicity, Inflammation and Genotoxicity

In line with the general scientific literature, the watersoluble tetrazolium salt (WST)-1 assay confirmed lower toxicity of the pristine amorphous SiO_2 (**Figure 5A**, EC ~40µg cm^{-2}) as compared to the pristine Ag Sigma (**Figure 5B**, EC ~20µg cm^{-2}). Furthermore, the results supported the working hypothesis that pre-treatment with artificial digestive fluids can modulate particle-induced effects depending on the material. Whereas pristine Ag Sigma significantly reduced THP-1 metabolic activity from 40µg cm^{-2} onwards, no effect was induced by PT particles (Figure 5B), which was confirmed in confluent intestinal epithelial cells, Caco-2 and E12. Again, PT Ag Sigma was less

cytotoxic than its pristine form (**Figure S3A**). The modulation of cytotoxic potential was highly limited on amorphous SiO_2 and did not result in significant differences (Figure 5A).

Having identified Ag Sigma as the ENM most sensitive to the GIT pre-treatment, we further investigated its inflammatory and DNA-damaging capacity. The release of cytokines from PMA-differentiated THP-1 cells shows a modulation of IL-8, IL-6 and TNF-α that is most prominent with prior activation of THP-1 cells by LPS/IFN-γ (**Figure 6**). The pre-activation of THP-1 cells was included to study a potential exacerbating effect of Ag Sigma in the context of ongoing inflammatory processes, which has previously been shown to affect ENM toxicity.[37] In the presence of GIT simulant fluids, the activation of THP-1 cells caused a significantly different release of IL-6 and TNF-α (Figure 6D & F). For concentrations up to 5.0μg cm^{-2}, the IL-6 release remained significantly different between pristine and PT Ag Sigma ENM. Regardless of the modification, the exposure resulted in a dose-dependent decrease of IL-6, which might in part be related to the corresponding cytotoxicity. A minimal dose-dependent increase in IL-8 was detected, which failed to reach statistical significance.

In the 3D liver spheroid model, neither the pristine Ag or PT Ag were shown to induce an elevated IL-8 response, nor a significant increase in TNF-α release. In fact, compared to the negative control, there was a significant reduction in IL-8 following 24hr exposure to the pristine Ag ENM which could be indicative of IL-8 inhibition. However, this reduction in IL-8 was not as prominent with the PT Ag ENMs, which were shown to induce an higher concentration of IL-8 release relative to the pristine particles, (**Figure 7A)**. This suggested that ENM transformation, as a result of the GIT pre-treatment scheme, may have an effect on the biological interaction of Ag ENMs and HepG2 spheroids. In addition, PT Ag ENMs induced higher TNF-α release in comparison to the untreated control, and a significant increase in TNF-α release compared to the pristine Ag material (**Figure 7B**). The trend across both IL-8 and TNF-α response suggested that pre-treating the ENMs in GIT simulant fluids followed by incubation with human blood plasma did increase the release of (pro-)inflammatory

mediators and could be influential in mediating an inflammatory response. IL-6 was also investigated, but all the results were found to be below dectable limits and so this cytokine not considered further (data not shown).

It is important to note that not all *in vitro* models and endpoints are sensitive to the transformations induced by the GIT pre-treatments that produce digested particles. Both viability and functionality of the liver spheroids appeared to be unaffected by exposure to Ag ENMs, regardless of whether the material was pristine or PT with the oral simulant fluids. There was no significant decrease in cell viability or the concentration of albumin present per liver spheroid, which further supported the observation that under these test conditions no cytotoxic response was elicited in the 3D HepG2 spheroids, even at Ag concentration of 10.0µg/mL. When genotoxicity was evaluated using the gold-standard *In Vitro* Micronucleus Assay (detects fixed chromsomal damage), it was only slightly higher following 24 hour exposure to the PT Ag ENMs than the pristine Ag ENMs. Hence, this induction of DNA damage did not reach significance (**Figure S4**). Furthermore, no significant induction of DNA damage was detected in Caco-2, but in E12 monocultures a significant difference of DNA damage was observed between pristine and PT Ag Sigma ENMs at 80µg/cm^2, using the Comet Assay (**Figure S3B**).

2.4 Positioning of concepts that increase realism in in-vitro testing

We expanded and critically assessed a concept to increase the realism of *in vitro* testing, by undertaking ENM pre-treatment in up to three sequential incubation steps *before* exploring cellular interaction, therefore designing a physiologically relevant exposure identity. The approach taken is analogous to OECD guidelines for the testing of non-particulate (molecularly dissolved) chemicals; *e.g.* the "Bacterial Reverse Mutation Test", OECD Test Guideline (TG) 471. TG471 specifies metabolization of the chemical, using enzymes and co-factors prior to toxicity testing as this process transforms the chemical identity of the test compound, and thus increases the realism of the test.

Previous studies have investigated the effects of physico-chemical changes on ENM-induced toxicity. However, the available outcomes do not yet allow for a general prediction, as the impact on their pathophysiology is dependent on the nature of the ENM, the specific modification as well as the cellular test system.[4,21,38] We addressed the evolving nature of ENM as they translocate through the body and demonstrated the implications for reactivity, cytotoxicity, inflammation and genotoxicity on differentiated, activated cells and cells from sites of secondary deposition, like the liver. With two nanoforms of both Ag and SiO_2, we found significant modulation of agglomeration and ion release, but for SiO_2 the incubation sequence did not matter and only one Ag ENM changed chemical speciation: Ag Sigma was oxidised and aggregated by the IUF GIT pre-treatment, resulting in modulation of its cytotoxic and pro-inflammatory potential, as well as a cell line-dependent reduction in DNA damage. The FRAS assay confirmed the reduction of ROS formation in abiotic conditions on pre-treated Ag Sigma due to its oxidation. In contrast, the modulation of physico-chemical properties and limited effect on the biological response for SiO_2 ENM suggested that pre-treatment could be an unnecessary complication when assessing the toxicological profile of some materials, even leading to interference from the chemicals in the pre-treatment simulants. As another dimension of increased realism, one could enrich the pre-treatment media by enzymes, bile salts, or food components.[39] Some of these interfere heavily with cell cultures. Some of these sequester ions and thus favor dissolution, which needs to be taken into account in risk assessment.[32] Here we focused on components and pH conditions that are essential to enable transformation of the particles. When proposing complex pre-treatment in tests of particle-induced effects,[40] future work should carefully compare effects of particles from complex digestion to less complex digestion or no digestion at all,[26] as demonstrated on four examples here.

3. Conclusions

To conclude, this study provides a physiologically relevant tiered testing strategy with which to assess the biological effects of ENM transformation that arise as the ENM traverse a cascade of biological

compartments. The present pre-treatments have been successfully implemented in three independent labs and can serve as standard protocols. Furthermore, the impact of such ENM pre-treatments upon toxicological outcomes at both the site of exposure (GIT) and a potential secondary organ of exposure (liver) have been demonstrated using advanced *in vitro* culture test systems. In addition, analogous pre-treatments to simulate pulmonary uptake were also demonstrated. However, we recommend that ENM pre-treatments in general or sequential incubations specifically are not performed routinely. Instead, a tiered approach can be implemented whereby a framework of transformation and reactivity, such as the scheme by Gray *et al* may prove useful to predict which material is sufficiently susceptible to transformation.[24] Following this, the physico-chemical transformation and reactivity would be assessed post pre-treatment in human cell-based systems, only if transformation is confirmed. By this rationale, zero-valent metals, which are colloidally unstable and have a tendency to oxidise, are particularly susceptible to irreversible transformation. For such materials, we consider the increased sources of error and variation by multiple simulant fluids to be sufficiently compensated by the increased realism of the exposure identity.

4. Experimental Section

Materials: We compared two polymer coated Ag ENM and two uncoated, amorphous silica ENM. PVP functionalized Ag Sigma was purchased from Sigma-Aldrich, Saint Louis, USA (Cat. No: 576832-5G). Fumed amorphous SiO_2 was purchased from Sigma (S5130). The constituent particles had a median size of 8.3nm (amorphous SiO_2), 35.5nm (SiO_2 NM200), 30.0nm (Ag Sigma) and 7.2nm (Ag NM300). The Ag NM300 was a suspension, whereas Ag Sigma was a powder. The SI reports TEM scans (Figure S1) and their complete physical-chemical characteristics (*e.g.* size, shape, crystallinity, surface chemistry by TEM, XRF, XRD, BET, XPS, zetapotential, TGA) (Table S2). Two materials (Ag NM300, SiO_2 NM200) came from the repository of the Joint Research Center (JRC) in Ispra, Italy, and served as benchmark for many European projects.

Standard Media: IUF_G, IUF_I, LSF and PSF simulant fluid composition (Figure 1) is detailed in the SI (Table S1). The two steps of the IUF protocol, IUF_G and IUF_I are listed as a combined treatment "IUF". The IUF GIT pre-treatment protocol explicitly states that no sonication should be used for sample preparation.

Sequential Incubation Standard Protocol: To simulate oral ENM exposure *in vivo*, 4.0 mg/mL of ENMs were incubated in IUF_G gastric simulant fluid (pH 2.7) for 30 mins at 37°C/5% CO_2, followed by a 30 min incubation in IUF_I intestinal simulant fluid (pH 9.5). For exposure scenarios (Table 1) that required an additional simulant fluid, the ENM were added to the first medium to obtain 4.0 mg/mL and stirred for 1hr at 350 rpm, 37 °C. The second medium (third medium, for the IUF_G and IUF_I sequence) was added in excess at a ratio of 10:1 to minimize influences (*e.g.* pH) of the previous medium.[32] The sample was then dispersed through ultrasonic power at an amplitude of 25% and a sonication duration of 1 min (Branson 550 (550W), Branson Ultrasonics Corp., Danbury, CT, USA). The sample size distribution was measured between and after all pre-treatments by Analytical Ultra Centrifugation[41] and dissolved ions measured with ICP-MS (Nexion 2000b, Perkin Elmer) following filtration (5kDa filter).

FRAS Assay: The assay was performed according to literature.[42] ENMs both with and without IUF GIT pre-treatment were incubated with human blood serum (HBS) and then separated from HBS *via* ultracentrifugation (AUC-Beckman XL centrifuge, Brea, USA). ENM-free HBS supernatant was incubated in the FRAS reagent, containing the Fe^{3+} complex. Total antioxidant depletion as a measure of the oxidative potential of ENMs was determined by UV-vis spectrum of the iron complex solution. Trolox (Vitamin E analogue) was used as an antioxidant to calibrate the FRAS results. Finally, the oxidative damage induced by ENMs was calculated in Trolox Equivalent Units (TEUs).

Gastrointestinal (GIT) Model and 3D In Vitro Hepatic Spheroid Models: A methodological description of the GIT and 3D hepatic models applied in this study, and their use for evaluating

cytotoxicity, (pro-)inflammatory response & genotoxicity are located in the Supplementary Information.

Acknowledgements

The authors acknowledge the funding received from the European Union's Horizon 2020 research and innovation program for the PATROLS project, under grant agreement No.760813.

References

1. Kreyling, W. G., M. Semmler-Behnke, J. Seitz, W. Scymczak, A. Wenk, P. Mayer, S. Takenaka, and G. Oberdörster. *Inhal Toxicol*, **2009**, *21.*
2. Lowry, G., Gregory, K., Apte, S. and Lead, J. *Environmental Science & Technology*, **2012**, *46(13)*, 6893.
3. Monopoli, M.P., Walczyk, D., Campbell, A., Elia, G., Lynch, I., Baldelli Bombelli, F., and Dawson, K.A. *J Am Chem Soc,* **2011**, *133,* 2525.
4. Tenzer, S., Docter, D., Kuharev, J., Musyanovych, A., Fetz, V., Hecht, R., Schlenk, F., Fischer, D., Kiouptsi, K., Reinhardt, C. and Landfester, K. *Nature nanotechnology*, **2013**, *8(10),* 772.
5. Milani, S., Baldelli Bombelli, F., Pitek, A.S., Dawson, K.A. and Radler, J. *ACS nano*, **2012,** *6(3),* 2532
6. Abbas, Q., Yousaf, B., Muhammad, U.-A., Munir, M.A.M., El-Naggar, A., Rinklebe, J. and Naushadi, M. *Environment International*, **2020**, *138*, 105646.
7. Fernando, I. and Zhou, Y. *Chemosphere*, **2019**, *216*, 297.
8. Wen, R., Hu, L., Qu, G., Zhou, Q. and Jiang, G. *NanoImpact*, **2016**, *2*, 18.
9. Walkey, C. and Chan, W. *Chem. Soc. Rev*., **2012**, *41(7),* 2780.
10. Akter, M., Sikder, M., Rahman, M., Ullah, A., Hossain, K., Banik, S., Hosokawa, T., Saito, T. and Kurasaki, M. *Journal of Advanced Research*, **2018**, *9*, 1.
11. Huk, A., Izak-Nau, E., el Yamani, N., Uggerud, H., Vadset, M., Zasonska, B., Duschl, A. and Dusinska, M. *Particle and Fibre Toxicology*, **2015**, *12(1).*
12. Piao, M., Kang, K., Lee, I., Kim, H., Kim, S., Choi, J., Choi, J. and Hyun, J., *Toxicology Letters*. **2011**. *201(1),* 92.
13. Sahu, S., Zheng, J., Graham, L., Chen, L., Ihrie, J., Yourick, J. and Sprando, R., *Journal of Applied Toxicology.* **2014**, *34(11)*, 1155.
14. Yao, Y., Zang, Y., Qu, J., Tang, M. and Zhang, T., *International Journal of Nanomedicine*. **2019**, *14*, 8787.
15. Zhu, B., Li, Y., Lin, Z., Zhao#, M., Xu, T., Wang, C. and Deng, N., *Nanoscale Research Letters.* **2016**, *11(1).*
16. Wallace, W.E., Vallyathan, V., Keane, M.J., and Robinson, V. *Journal of Toxicology and Environmental Health*. **1985**, *16(3 – 4)*, 415.

17. Luoto, K., Holopainen, M., Karppinen, K., Perander, M., and Savolainen, K. *Environmental health perspectives*. **1994**, *102(5)*, 103.
18. Phillips, B.J., Kranz, E., Elias, P.S., and Münzner, R. *Food and Cosmetics Toxicology.* **1980***, 18(4),* 371.
19. Oomen, A.G., Hack, A., Minekus, M., Zeijdner, E., Cornelis, C., Schoeters, G., Verstraete, W., Van de Wiele, T., Wragg, J., Rompelberg, C.J.M., Sips, A.J.A.M, and Van Wijnen, J.H. *Environmental Science Technology.* **2002***, 36(15),* 3326.
20. Walczak, A.P., Fokkink, R., Peters, R., Tromp, P., Herrera Rivera, Z.E., Rietjens, I.M.C.M., Hendriksen, P.J.M., and Bouwmeester, H. *Nanotoxicology*. **2012**, *7(7)*, 1198.
21. Gerloff, K., Pereira, D.I.A., Faria, N., Boots, A.W., Kolling, J., Förster, I., Albrecht, C., Powell, J.J., and Schins, R.P.F. *Nanotoxicology*. **2013**, *7(4),* 353.
22. Cai, X., Liu, X., Jiang, J., Gao, M., Wang, W., Zheng, H., Xu, S. and Li, R. *Small*. **2020**, 1907663.
23. Abdelkhaliq, A., van der Zande, M., Undas, A.K., Peters, R.J., Bouwmeester H. *Nanotoxicology.* **2020**, *14 (1)*, 111.
24. Gray, E., Browning, C., Wang, M., Gion, K., Chao, E., Koski, K., Kane, A. and Hurt, R. *Environmental Science: Nano.* **2018**, *5(11)*, 2545.
25. Hellack, B., Nickel, C., Albrecht, C., Kuhlbusch, T.A.J., Boland, S., Baeza-Squiban, A., Wohlleben, W. and Schins, R.P.F. *Environmental Science: Nano*. **2017**, *4(10),* 1920.
26. Kämpfer, A., Busch, M. and Schins, R., Chemical Research in Toxicology. **2020***, 33(5),* 1163.
27. Kermanizadeh, A., Brown, D., Moritz, W. and Stone, V., Scientific Reports. **2019**, *9(1).*
28. Llewellyn, S. V., Conway, G.E., Shah, U., Evans, S.J., Jenkins, G.J.S., Clift, M.J.D., and Doak, S.H *Protocol. J. Vis. Exp. (In-press).* **2020**, *160*, 61141.
29. Bihari, P., M. Vippola, S. Schultes, M. Pr„tner, A. G. Khandoga, C. A. Reichel, C. Coester, T. Tuomi, M. Rehberg, and F. Krombach. , *Particle and Fibre Toxicology*. **2008**, *5,* 14.
30. Schulze, C., A. Kroll, C. M. Lehr, U. F. Schufer, K. Becker, J. Schnekenburger, C. Schulze-Isfort, R. Landsiedel, and W. Wohlleben. Nanotoxicology. **2008***, 2*, 51.
31. Bove, P., Malvindi, M. A., & Sabella, S. *Journal of Physics: Conference Series.* **2017**, *838*, 012003.
32. Bove, P., Malvindi, M., Kote, S., Bertorelli, R., Summa, M. and Sabella, S., *Nanoscale*. **2017**, *9(19),*6315.
33. Walczyk, D., Bombelli, F., Monopoli, M., Lynch, I. and Dawson, K., *Journal of the American Chemical Society.* **2010**, *132(16),* 5761.
34. Wohlleben, W. *Journal of Nanoparticle Research*. **2012**, *14(12)*.
35. Braun, K., A. Pochert, M. Beck, R. Fiedler, J. Gruber and M. Lindén. *Journal of Sol-Gel Science and Technology*, **2016**, *79(2)*, 319.
36. Izquierdo-Barba, I., M. Colilla, M. Manzano and M. Vallet-Regí. *Microporous and Mesoporous Materials*, **2010**, *132(3),* 442.
37. Kämpfer, A., Urbán, P., La Spina, R., Jiménez, I., Kanase, N., Stone, V. and Kinsner-Ovaskainen, A. *Toxicology in Vitro.* **2020**, *63*, 104738.

38. Lemarchand, C., Gref, R., Passirani, C., Garcion, E., Petri, B., Müller, R., Costantini, D. and Couvreur, P. *Biomaterials*. **2006**, *27(1),* 108.
39. Sohal, I. S., Y. K. Cho, K. S. O'Fallon, P. Gaines, P. Demokritou and D. Bello. *ACS Nano.* **2018**, *12(8),* 8115.
40. Sohal, I. S., G. M. DeLoid, K. S. O'Fallon, P. Gaines, P. Demokritou and D. Bello. *NanoImpact.* **2020**, *17*, 100209.
41. Mehn, D., Rio-Echevarria, I., Gilliland, D., Kaiser, M., Vilsmeier, K., Schuck, P. and Wohlleben, W. *NanoImpact.* **2018**, *10*, 87.
42. Gandon, A., Werle, K., Neubauer, N., Wohlleben, W. *J. Phys. Conf. Ser*. **2017**, *838*, 012033.
43. Thongkam, W., Gerloff, K., van Berlo, D., Albrecht, C. and Schins, R. *Mutagenesis*. **2016**. *32(1)*, 105.
44. Kinsner, A., M. Boveri, L. Hareng, G. C. Brown, S. Coecke, T. Hartung, and A. Bal-Price., *J. Neurochem.* **2006**. *99,* 596.

Figures and Tables

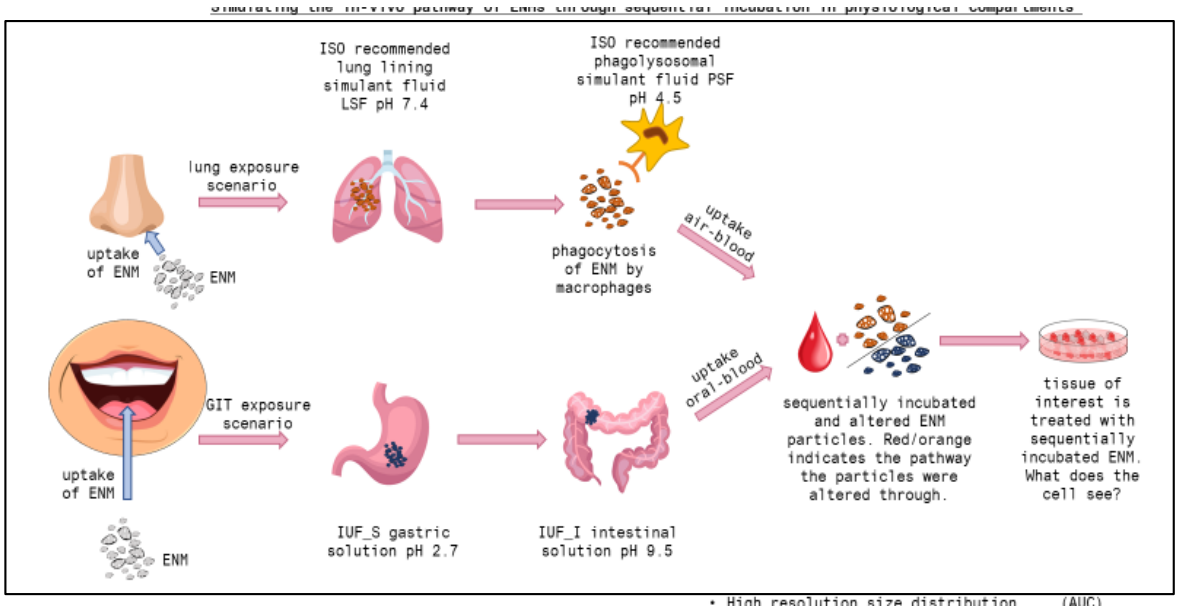

Figure 1: Simulant fluid pre-treatments enable design of the *in vitro* exposure identity to better represent the identity of the particle that reaches the target tissue after a journey through several physiological compartment. This schematic provides an overview of the incubation of test particles in at least two simulant media, and optionally also incubated in blood serum, before they are finally exposed to human cells *in vitro*. GIT – Gastrointestinal Tract.

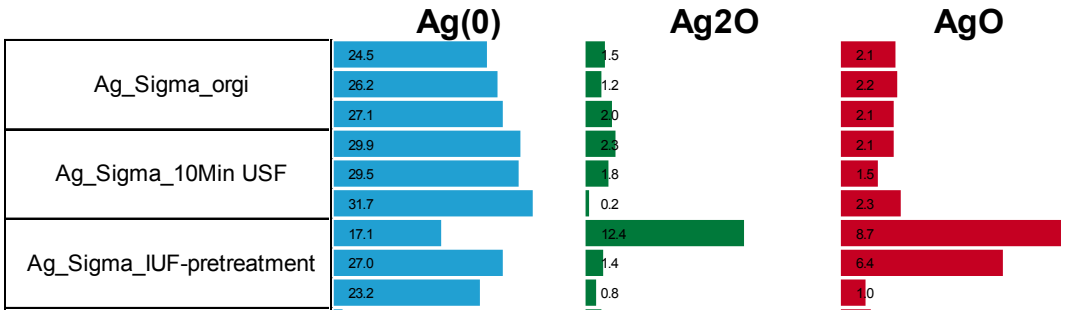

Figure 2: XPS analysis of transformation induced by the IUF (=IUF_G + IUF_I) GIT pre-treatment of Ag Sigma. The results represent triplicate testing, and the small numbers report the atom-% composition of the surface. As controls, the materials are analysed in the original state (no dispersion), and after dispersion in deionized water with sonication. The IUF GIT pre-treatment does not use sonication, but simulates a chemically aggressive biological compartment. In the SI, results of the XPS analysis on a widely studied reference material Ag NM300 from the JRC repository, demonstrate that only the Ag Sigma material is originally present as metallic Silver, whereas the Ag NM300 is already oxidized before the treatment.

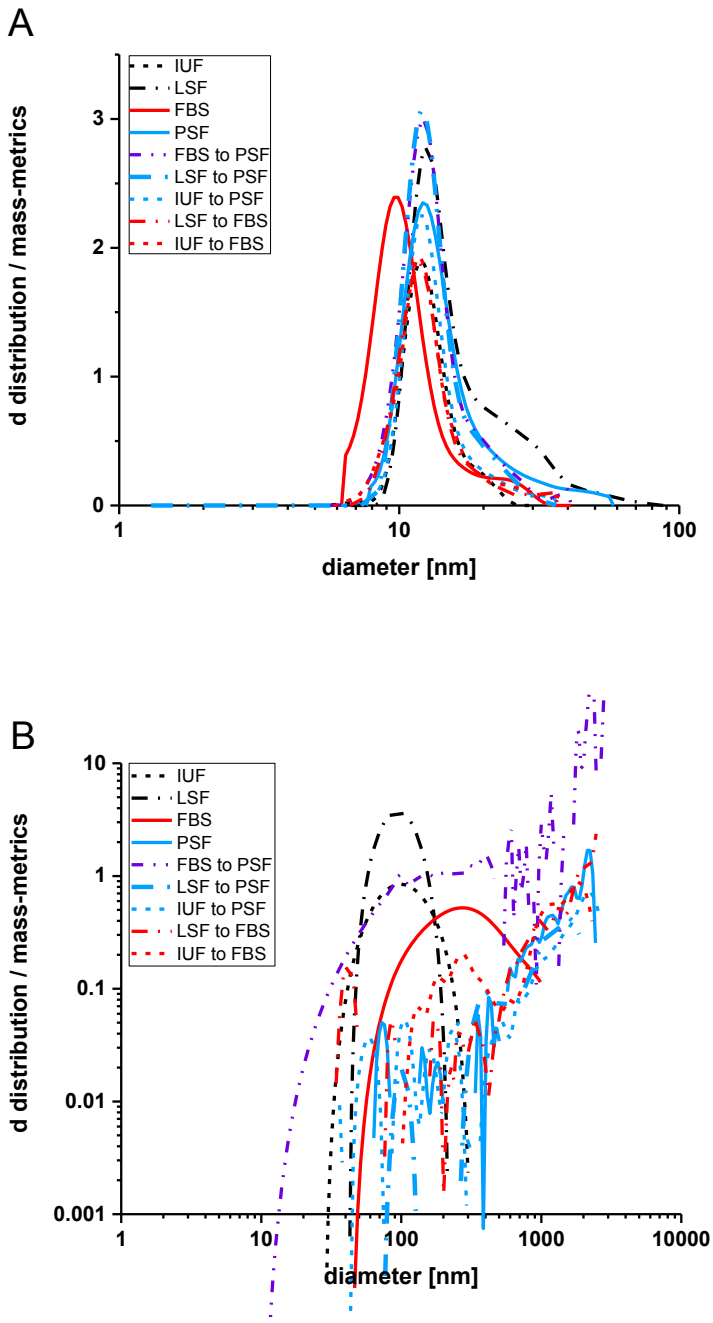

Figure 3: Size distributions after single or sequential incubations for (A) Ag NM300 and (B) SiO_2 amorphous. In both, A and B, the black dashed curve corresponds to pre-treatment in the IUF simulant fluids; black dashed curve with dots represents pre-treatment in LSF; red solid curve represents pre-treatment in FBS; blue solid curve represents pre-treatment in PSF; purple dashed curve with dots represents pre-treatment in FBS followed by PSF; blue dashed curve with dots represents pre-treatment in LSF followed by PSF; blue dashed curve represents pre-treatment in IUF simulant fluid followed by PSF; red dashed curve with dots represents pre-treatment in LSF followed by FBS; and the red dashed curve represents pre-treatment in IUF simulant fluids followed by FBS. The D50 median sizes from all cascaded pretreatments are given in Tables S5.

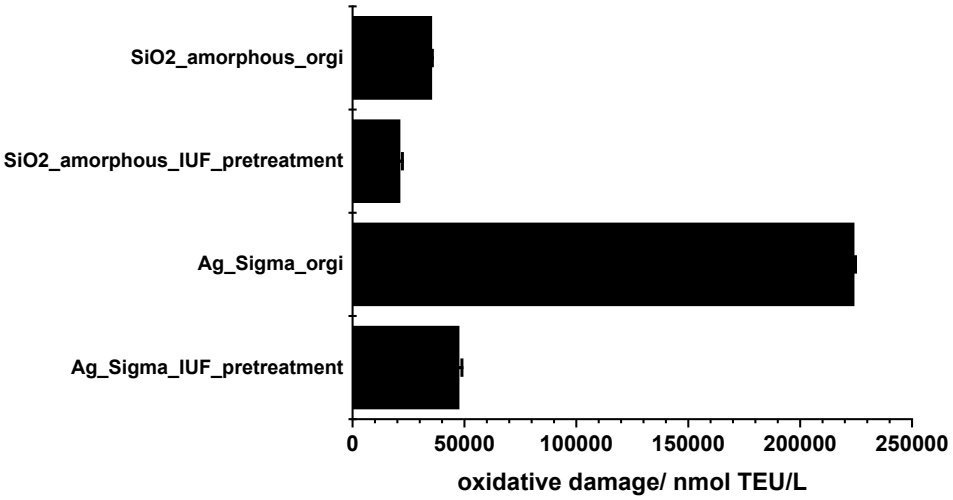

Figure 4: FRAS results on amorphous SiO_2 and Ag Sigma without (orgi) and with the IUF GIT pre-treatment.

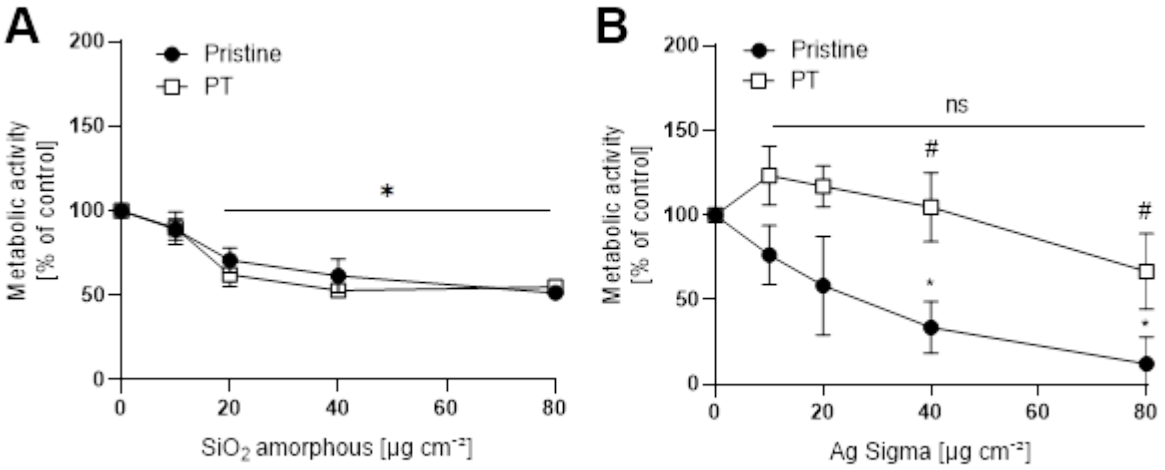

Figure 5: Metabolic activity after 24h exposure to (A) amorphous SiO_2, (B) Ag Sigma in PMA-differentiated THP-1 cells. Average ± SD, N≥3 displayed; *$p \leq 0.05$* compared to the corresponding control; #$p \leq 0.05$ compared to the corresponding concentration of pristine ENM by One-way ANOVA and Tukey's post hoc test.

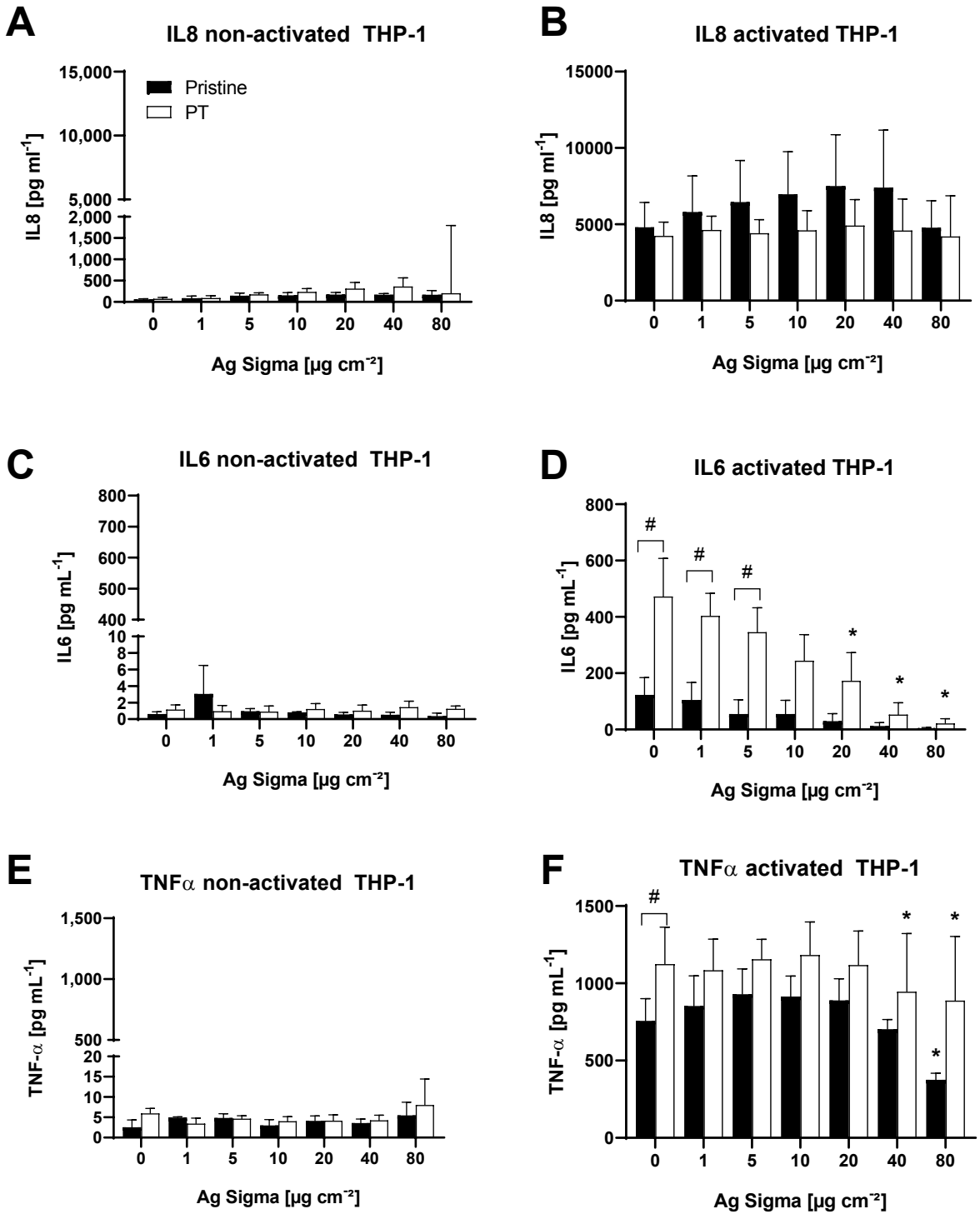

Figure 6: Release of (A&B) IL-8, (C&D) IL-6 and (E&F) TNF-α after 24hr exposure to pristine or PT Ag Sigma ENM in PMA-differentiated (non-activated) THP-1 cells (A,C,E) and PMA-differentiated, LPS/IFNγ-activated THP-1 cells. Average ± SD, N=3 displayed; *$p \leq 0.05$ compared to the respective unexposed control; #$p \leq 0.05$ compared to the corresponding concentration of pristine Ag Sigma-PVP ENM by Two-way ANOVA and Tukey's *post hoc* test.

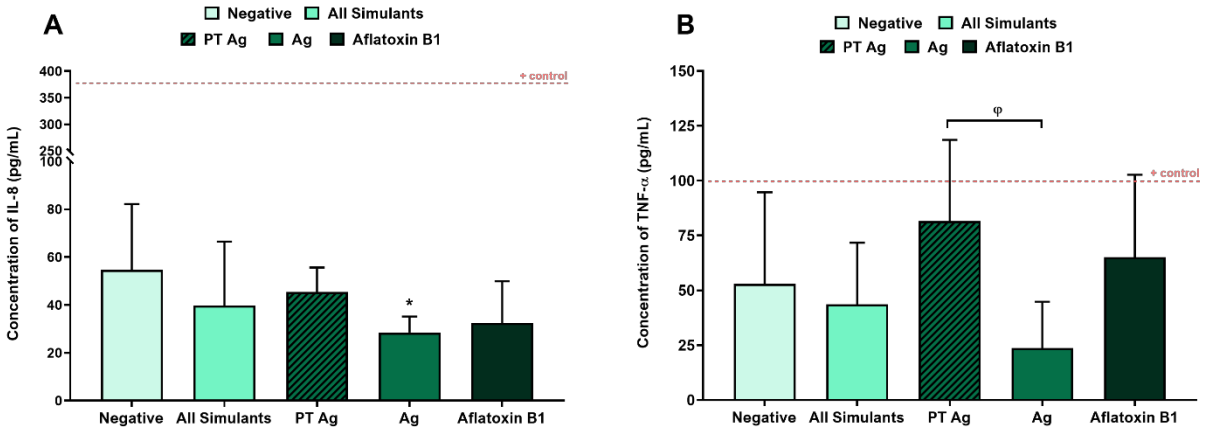

Figure 7: Release of (pro-)inflammatory mediators following exposure of 3D liver spheroid models to both pristine ENMs and ENMs PT with GIT simulant fluids followed by incubation in human blood plasma. (A) IL-8 release after 24 hour Ag ENM exposure, (B) TNF-α release after 24 hour Ag ENM exposure, to both pristine and PT Ag ENMs. An untreated, media only sample was used as the negative control whilst 0.1µM of Aflatoxin B1, a known liver carcinogen, was used as a chemical control for genotoxicity. Mean data of three biological replicates, analysed in triplicate (n=9) are presented ± SD. Red dotted line represents the mean positive control response induced by 0.25µg/mL of TNF-α protein (NBP2-35076-50ug, Biotechne, UK). Significance indicated in relation to the negative control: * = $p \leq 0.05$ with significance between groups indicated as: φ = $p \leq 0.05$.

Table 1: *In vivo* journey emulated by sequential incubation in physiologically relevant simulant fluids.

Simulant fluids utilized in sequential incubation	Simulated *in vivo* passage
Emulating Oral ENM Exposure	
IUF_G to IUF_I: (*noted as "IUF" in graphs & tables*)	Gastric compartments, stomach to the intestine.
IUF to FBS:	Gastric compartments before uptake through intestinal barrier into blood and systemic circulation.
FBS to PSF:	Systemic circulation in serum, then uptake into a lysosome *e.g.* by Kupffer cells in Liver.
IUF to PSF:	Gastric compartments before uptake through the intestinal barrier into the blood, prior to eventual uptake into a lysosome, *e.g.* by Kupffer cells in Liver.[1]
Emulating Inhalation ENM Exposure	
LSF to PSF:	Deposition in alveolar lung lining fluid, then uptake by macrophages into lysosome (*i.e.* first step of clearance).
LSF to FBS:	Deposition in alveolar lung lining fluid, then uptake through air-blood-barrier into the blood and systemic circulation.

[1] As this already requires three sequential incubations, and considering that serum is least relatively influential, we skip the intermediate incubation in FBS that would simulate the phase of systemic circulation.

Table 2: Particle size median (D50) after normalization to the median size distribution when dispersed directly into the second medium. The color code is normalized on the entire data set to highlight cases where the sequential incubation leads to results that have very similar (white), lower (blue) or higher (red) levels of agglomeration as compared to single incubation in either the first or the second medium of the sequence.

		Relative to 1st medium	Relative to 2nd medium
Ag Sigma	IUF_G to _I	65%	110%
	FBS to PSF	57%	7%
	IUF to FBS	620%	954%
	LSF to PSF	147%	111%
	LSF to FBS	30%	192%
	IUF to PSF	641%	114%

		Relative to 1st medium	Relative to 2nd medium
SiO_2 amorphous	IUF_G to _I	12%	105%
	FBS to PSF	826%	135%
	IUF to FBS	1273%	475%
	LSF to PSF	1259%	73%
	LSF to FBS	1818%	643%
	IUF to PSF	1714%	104%